Equatorward moving auroral signatures of a flow burst observed prior to auroral onset

L. Kepko,[1] E. Spanswick,[2] V. Angelopoulos,[3] E. Donovan,[2] J. McFadden,[4] K.-H. Glassmeier,[5] J. Raeder,[1] and H. J. Singer[6]

Received 23 October 2009; revised 20 November 2009; accepted 30 November 2009; published 31 December 2009.

[1] We present observations of a substorm that occurred on February 25, 2008. Auroral onset was observed with a multi-spectral (λ = 427.8, 557.7 and 630.0 nm) and white light all sky imager at Gillam, Canada. An equatorward moving diffuse auroral patch was observed in the λ = 630.0 nm images at least six minutes prior to auroral onset. This form emerged from the background noise poleward of the eventual onset arc and intensified as it moved equatorward. Auroral expansion onset occurred when this form reached the onset arc location. Flows were detected by THEMIS probes P3 (TH-D) and P4 (TH-E) near $X \sim -11\ R_E$ nearly 90 seconds prior to auroral expansion. A small discrete arc was observed in the λ = 557.7 nm images at the westward and equatorward edge of the diffuse 630.0 nm patch nearly 2 minutes prior to expansion onset, suggesting a field-aligned current of a substorm current wedge geometry. We conclude that the equatorward moving λ = 630.0 nm diffuse auroral patch was generated by processes associated with an earthward moving flow burst that formed prior to auroral substorm onset. **Citation:** Kepko, L., E. Spanswick, V. Angelopoulos, E. Donovan, J. McFadden, K.-H. Glassmeier, J. Raeder, and H. J. Singer (2009), Equatorward moving auroral signatures of a flow burst observed prior to auroral onset, *Geophys. Res. Lett.*, *36*, L24104, doi:10.1029/2009GL041476.

1. Introduction

[2] The near-Earth neutral line (NENL) model postulates that magnetic reconnection in the midtail plasmasheet is the first event in the expansion phase of a magnetospheric substorm, preceding near-Earth current disruption and dipolarization, Pi2 pulsations, and auroral arc brightening [*Baker et al.*, 1996]. Observations have shown that the onset arc occurs near the most equatorward boundary of auroral activity and that this region maps to the near-geosynchronous (6–10 R_E) region [*Elphinstone et al.*, 1991; *Samson et al.*, 1992]. Because magnetic reconnection is observed further downtail this requires that the reconnection site and the discrete onset aurora are not magnetically linked. Instead, it has been suggested that flow braking and diversion near the transition between stretched tail and dipolar field lines is the source of energy for auroral onset [e.g., *Shiokawa et al.*, 1998]. Simulations support this interpretation and show that the strong currents required for discrete auroral arc formation are created in the region of dipolarization, away from the reconnection site [*Birn and Hesse*, 1996]. This revision of the NENL model helped to reconcile the observed auroral onset location with reconnection in the midtail plasmasheet as the cause of substorm onset.

[3] Despite this progress, the lack of an auroral signature poleward of the onset arc prior to onset has been a major criticism of the NENL model. A flow burst traveling from a reconnection site in the midtail plasmasheet will take several minutes to advect to the flow braking region. Yet during this time, prior to auroral onset, there have been no reported visible manifestations of this flow in the ionospheric data. In this paper we present an event that may help resolve this apparent inconsistency. We present an event from 2008 using multi-spectral all sky imager [*Donovan et al.*, 2003] and the THEMIS white light imager [*Mende et al.*, 2008] data from Gillam and in-situ plasma [*McFadden et al.*, 2008] and magnetic field [*Auster et al.*, 2008] data from the THEMIS satellites [*Angelopoulos*, 2008]. The multispectral data show a broad patch of diffuse λ = 630.0 nm aurora that moved equatorward towards the ensuing onset arc at least 6 minutes prior to auroral substorm onset. This patch was not observed in the ground-based THEMIS white light images. When this auroral patch reached the equatorward auroral boundary the onset arc formed and an auroral substorm commenced. The THEMIS satellite data show fast Earthward flows prior to auroral onset, but after the diffuse auroral patch was first detected. The results support *Angelopoulos et al.*'s [2008] conclusion that substorm onset is initiated by a flow burst and for the first time identifies a visual ionospheric signature of a flow burst prior to auroral onset.

2. Data

[4] The event occurred on February 25, 2008, near 0530 UT. THEMIS probes P3 (TH-D) and P4 (TH-E) were located pre-midnight at (x, y) = (−11.1, 2.1) and (−10.6, 2.9) R_E in GSM coordinates, and GOES-12 was at geosynchronous post-midnight. The ionospheric footprints of the spacecraft mapped along field lines using the T01 model [*Tsyganenko*, 2002] are shown in the top left image of Figure 1. The field-line mapping places the THEMIS probes near the local time of Gillam and poleward of the auroral

[1]Space Science Center, University of New Hampshire, Durham, New Hampshire, USA.
[2]Department of Physics and Astronomy, University of Calgary, Calgary, Alberta, Canada.
[3]Institute of Geophysics and Planetary Physics, University of California, Los Angeles, California, USA.
[4]Space Sciences Laboratory, University of California at Berkeley, California, USA.
[5]Institute of Geophysics and Extraterrestrial Physics, Technical University of Braunschweig, Braunschweig, Germany.
[6]Space Weather Prediction Center, NOAA, Boulder, Colorado, USA.

0094-8276/09/2009GL041476$05.00

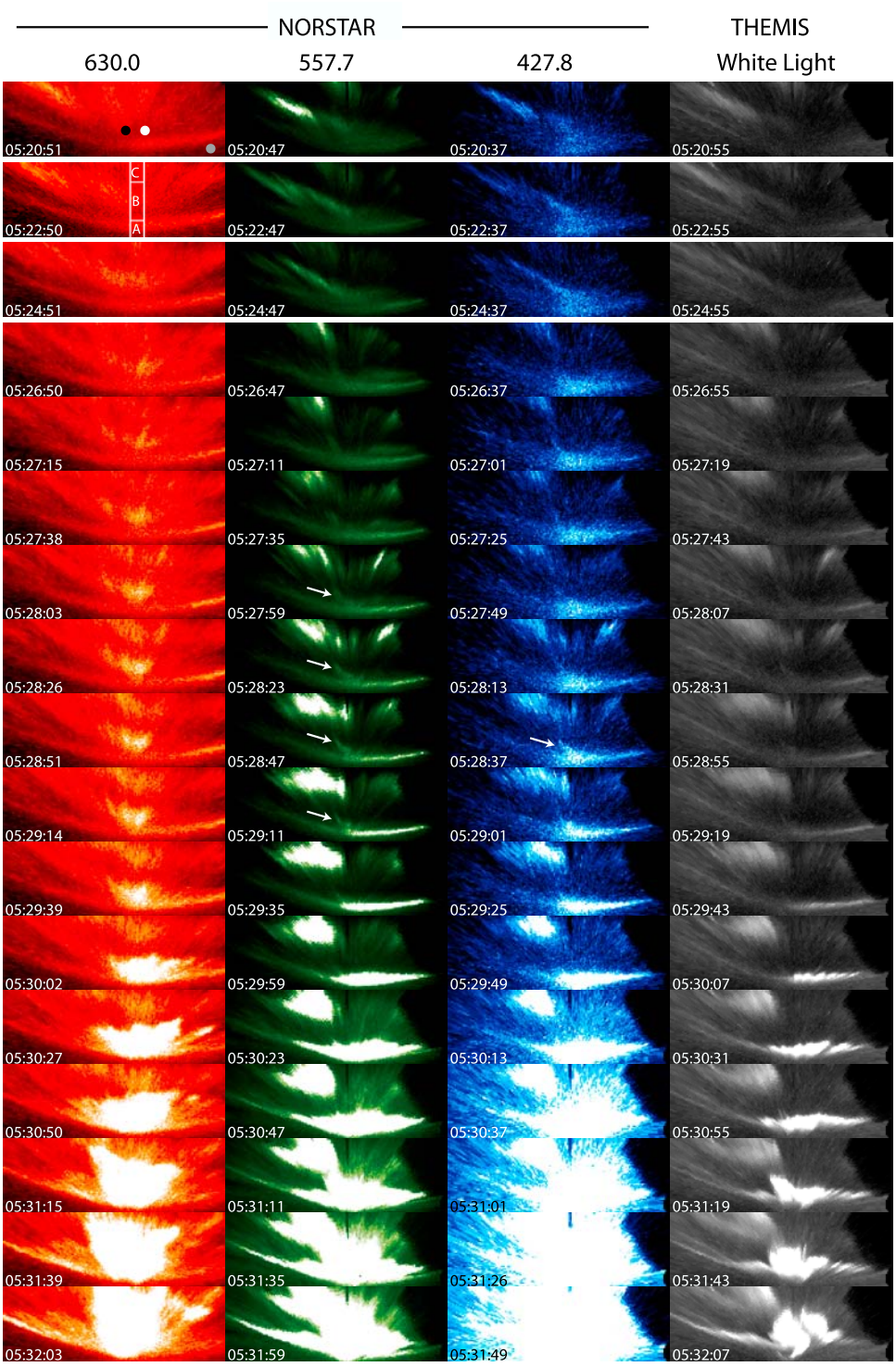

Figure 1. Images from the multispectral all-sky and THEMIS white light cameras at Gillam. Images have been cropped to about 1/4 the field of view in the north-south direction. The raw images have been projected onto geographic coordinates, with dark frame subtracted. North is up and west to the left, and the perspective is above the Earth looking down. The positions of P3 (black), P4 (white) and GOES-12 (grey) are marked with circles in the upper left image and mapped as described in the text. The letters A-C represent the low (A), mid (B) and high (C) latitude auroral features. The vertical white lines show the width over which the intensities of Figure 2 were calculated, while the horizontal lines mark the north-south cutoffs used in Figure 3a.

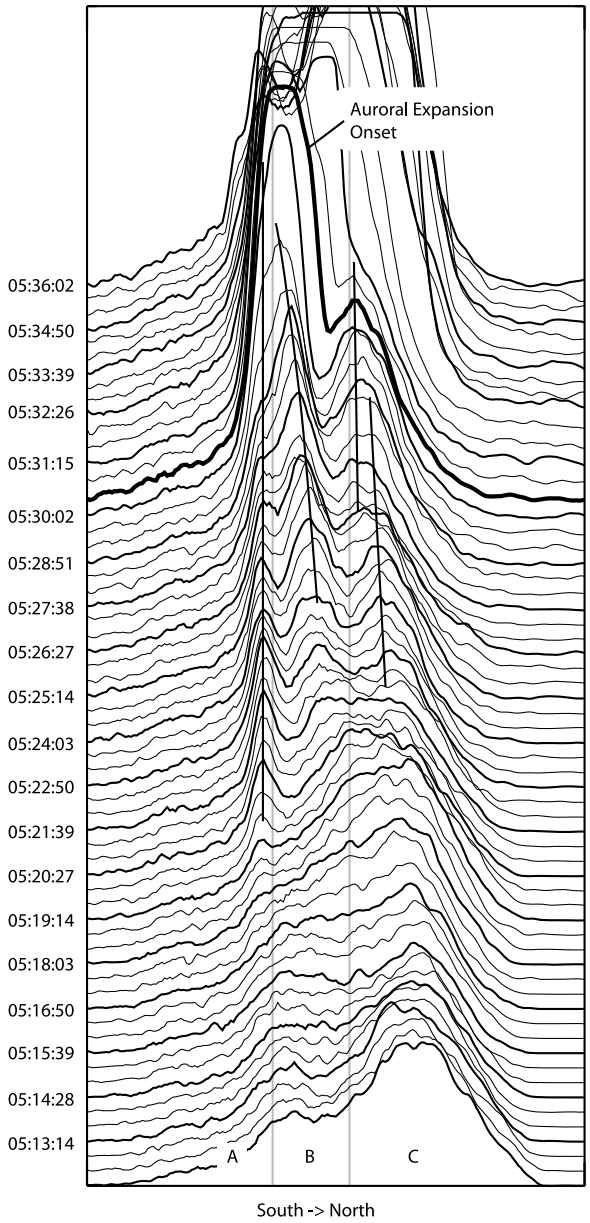

Figure 2. Stackplot of north-south slices of λ = 630.0 nm images. The images in Figure 1 were averaged over 11 pixels in longitude and 3 pixels in latitude to produce this plot. The letters A-C represent the low (A), mid (B) and high (C) latitude auroral features as in Figure 1. The thick line marks the image nearest auroral expansion onset.

onset location. The GOES-12 footprint lies equatorward and east of the onset. Different mapping models do not significantly alter the local time of the mapping.

[5] Images from the all-sky multispectral imager and the THEMIS white light imager at Gillam are shown also in Figure 1. The four columns represent data from three wavelengths, λ = 630.0 (red), 557.7 (green), and 427.8 (blue) nm, and white light. The different auroral wavelengths respond to different energy ranges of electron precipitation. The λ = 630.0 nm band is sensitive to low energy (<1 keV) electrons [*Rees and Roble*, 1986] while λ = 557.7 nm emissions are produced by an incident electron flux of >~1 keV [*Sharp et al.*, 1983]. The λ = 427.8 nm emission (N_2^+) is correlated with the energy of the precipitating electrons, and an increase in brightness often indicates an increase in precipitating electron energy [*Eather and Mende*, 1971]. We have cropped the all-sky images to focus on the active aurora region. The images show three areas of auroral activity, labeled A, B and C in the second λ = 630.0 nm image. At the equatorward edge Gillam observed in all wavelength channels a narrow, stable auroral structure (A). Gillam observed also intermittent high latitude activity (C), most clearly in the 557.7 nm images.

[6] The λ = 630.0 nm images show a diffuse equatorward moving patch (B) that grew out of the background just equatorward of the high latitude activity. This patch moved slowly equatorward until it reached the equatorward auroral structure (A) and an auroral expansion occurred (0530:31 UT). Note the difference between the 0527:15 UT image, which shows a clear gap between the patch and the equatorward boundary, and the 0529:14 UT image, where the equatorward edge of the patch appears to have merged into the equatorward boundary. Starting near 0526:47 UT a narrow discrete form was observed in the λ = 557.7 nm wavelength images (marked with an arrow), and appears to lie near the westward edge of the diffuse redline patch. This small, discrete arc moved equatorward and merged into the equatorward boundary just prior to auroral expansion onset. Although less clear, the 427.8 nm emissions showed the same structure (see especially 0528:37 UT). The white light images show the formation of auroral rays at 0529:43, auroral beads at 0530:07, and expansion and break-up near 0530:31 UT.

[7] Figure 2 shows a stackplot of λ = 630.0 nm average intensity along a north-south strip centered on the onset meridian (marked with vertical white lines in Figure 1). This representation of the data shown in Figure 1 highlights the equatorward motion of the diffuse auroral patch, and the relative stability of the equatorward structure. It shows also that the diffuse redline form grew out of the background noise in the area between the activity at high latitude and the equatorward auroral boundary. In combination with the images we have identified 0523:15 UT as the time at which we can unambiguously identify a persistent diffuse auroral patch rising out of the background.

[8] Figure 3a shows the north-south location of the peak intensity in three north-south windows (white boxes in Figure 1) covering the auroral features identified in Figures 1 and 2. Points are connected when the peak intensities can unambiguously be identified with the same auroral feature. The equatorward motion and growth in brightness of the diffuse auroral patch (B) is evident. The ground magnetic field data shown in Figures 3b and 3c show that the substorm current system formed when this form reached the equatorward boundary, and confirms that the onset arc formed north of Gillam. The Gillam magnetometer measured a negative B_z deflection (positive z downward), while Fort Churchill measured an initial positive B_z deflection. This places the ionospheric portion of the substorm current wedge between the two stations, consistent with the auroral observations. As the substorm progressed Fort Churchill measured a negative B_x (southward) deflection as the B_z perturbation changed sign from positive to

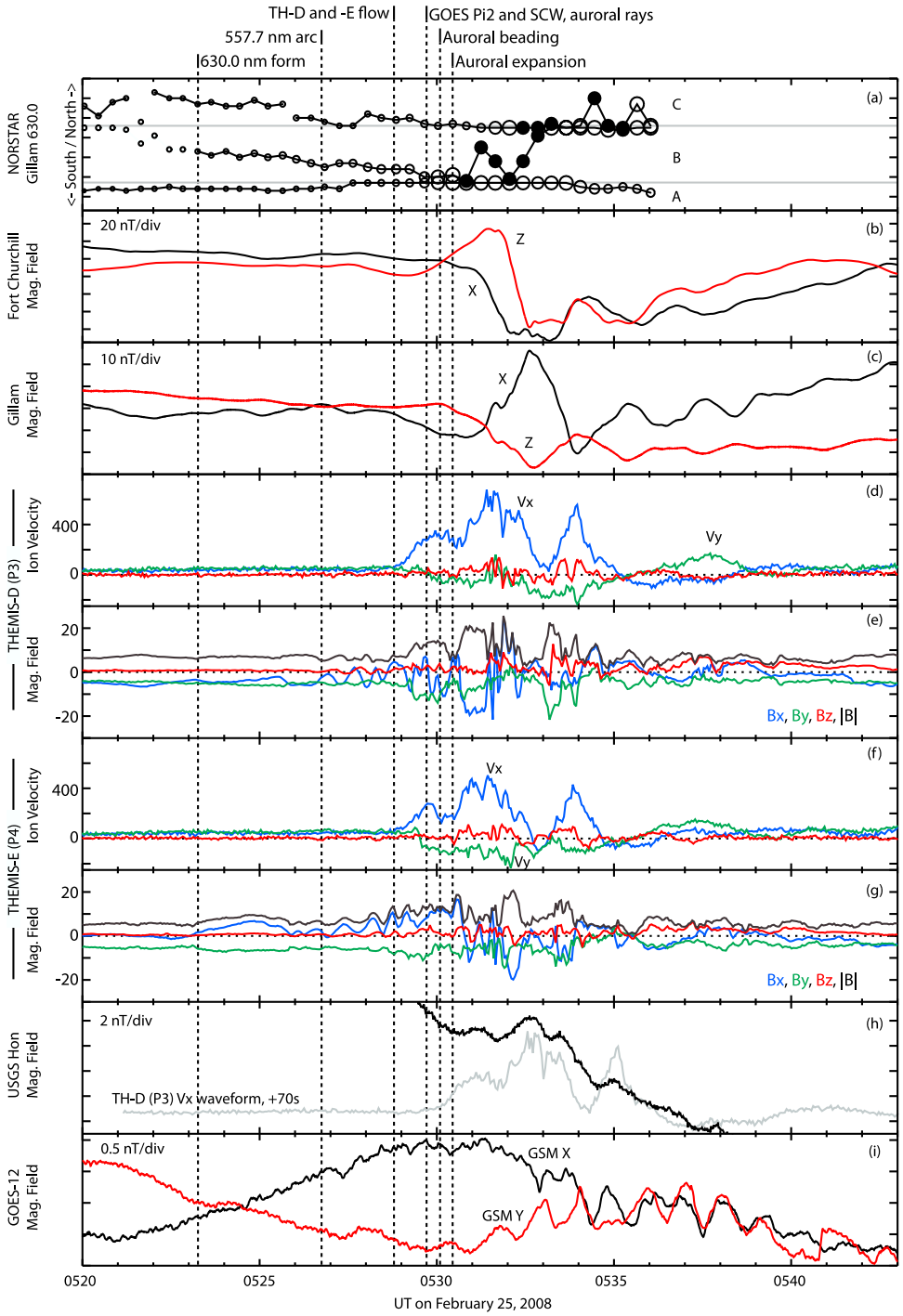

Figure 3. (a) North-South ASI pixel position of the peak intensity from Figure 2 of the $\lambda = 630.0$ nm of the three auroral regions identified in the text. Points are connected when they can be identified with the same auroral feature. Circles correspond to brightness, with filled circles identifying saturation. The X (positive North) and Z (positive down) magnetometer data, with background subtracted, from (b) Fort Churchill (327.3° E, 68.30° N, geomagnetic) and (c) Gillam (331.0° E, 67.1° N). THEMIS probes (d and e) P3 and (f and g) P4 plasma velocity and magnetic field data; (h) Honolulu X component magnetometer data; (i) GOES-12 X and Y GSM magnetic field data, with background subtracted.

negative, indicating that the westward electrojet moved poleward, consistent with poleward expansion.

[9] The THEMIS in situ observations are shown in Figures 3d–3g. Both spacecraft were located near the central plasmasheet for the majority of the event. Plasma flow was first detected at 0528:50 UT. Prior to this time both spacecraft observed low-speed flow moving earthward and duskward. Both probes observed similar variations of the flow, despite being separated by ~1 R_E in azimuth. This suggests a coherence of the flow channel of at least this

Table 1. Time Sequence of Events for the February 25, 2008 Substorm

Time	Event
0523:15	Brightness increase in 630.0 nm emissions
0526:47	Small arc in 427.8 and 577.7 nm forms
0528:50	Flow observed at P4 and P5 (11 RE)
0529:11	Brightening of equatorward boundary begins
0529:45	Pi2 and dipolarization at GOES-12 (6.6 RE)
	Auroral rays observed in white light
0530:07	Auroral beading
0530:31	Auroral expansion
0530:38	Flank, low-latitude Pi2

length scale. There was slight dipolarization of the magnetic field observed at the locations of both probes. GOES-12 was located just post-midnight and observed Pi2 pulsations and magnetic field dipolarization beginning near 0529:45 UT. GOES-11, located west of the onset meridian, observed Pi2 also, but at a smaller amplitude (not shown).

3. Discussion

[10] A summary of the timing of the observed phenomenological and intensity changes is shown in Table 1 and at the top of Figure 3. Of particular interest is the formation of an equatorward moving patch of diffuse λ = 630.0 nm aurora at least 6 minutes prior to auroral substorm onset. We assert that this auroral form represents the ionospheric footprint of an Earthward moving flow burst in the midtail plasmasheet, although the exact linkage is unclear. *Rees and Roble* [1986] showed that an incident Maxwellian electron spectrum with a characteristic energy of 0.1 keV and total energy-input rate of 1 erg/s/cm^2 can produce a significant emission in the λ = 630.0 nm band. Additionally, the λ = 630.0 nm emission is a high altitude emission (typically taken to be 230 km [*Sharp et al.*, 1979]). The enhanced λ = 630.0 nm emissions for this event indicate a combination of increased number flux and/or increased characteristic energy of the incident electrons. This in turn could mean enhanced scattering of electrons in the plasmasheet, increased energy (heating) of the precipitating electrons, demand for upward current over a broad ionospheric region, or Alfvénic acceleration above the auroral zone [e.g., *Mende et al.*, 2003]. Without a direct measurement of the precipitating particles, we cannot argue definitively for one process over another.

[11] The emissions from λ = 557.7 and λ = 427.8 nm exhibit a different behavior. These wavelength emissions are generated by higher energy particles, and more typically associate with discrete auroral arcs as opposed to scattered plasmasheet particles. The images shown in Figure 1 indicate that discrete auroral emissions formed near 0526:47 UT, at least 3 minutes after the first indication of brightening in the λ = 630.0 nm emissions. Further, the emissions were structured, appearing as a small arc slanted slightly relative to the equatorward boundary, rather than the diffuse patch indicated in λ = 630.0 nm. The discrete structure suggests upward field-aligned current, and the location on the western edge of the of the λ = 630.0 nm patch is consistent with proposed current systems of earthward traveling flow bursts [e.g., *Kepko et al.*, 2004]. Another possibility is that the small arc is related to increased flow diversion and magnetic shear ahead of the flow as it nears the inner magnetosphere, leading to strong field-aligned currents [e.g., *Birn and Hesse*, 1996].

[12] Flow was detected at the THEMIS probes at 0528:45 UT, increasing to greater than 100 km/s by 0529:00 UT. By 0530:00 UT this first flow burst had reached a peak of V_x = 300 km/s. If the flow had maintained this constant speed this places the origination of the flow near $X \sim -28$ RE (300 km/s $\times$ 6 minutes). The slow duskward flow observed prior to the event is likely enhanced diamagnetic flow associated with the growth phase. The high-latitude auroral activity (C) most likely corresponds to activity near the distant X-line. This provides an outer boundary location relative to the location of a new X-line that may have formed prior to auroral onset. Both Figures 1 and 2 show that the diffuse form grows out of the noise equatorward of this high-latitude activity.

[13] Much previous literature [e.g., *Elphinstone et al.*, 1991; *Samson et al.*, 1992] has established that the onset arc maps to the area near the transition between stretched tail-like and dipolar-like field lines. The in situ observations are consistent with the mapping for this event, which places the THEMIS probes tailward and GOES earthward of this transition region. The GOES spacecraft detected currents and transient response Pi2 associated with the substorm current wedge near 0529:45 UT, one minute after THEMIS (near $X = -11$ R_E) measured increased earthward plasma flow. The one minute delay is consistent with the motion of the flow burst a further 3 R_E earthward (300 km/s $\times$ 60 s), and a location of the braking region near 8 R_E. The Pi2 observed at Honolulu (Figure 3h) provides further evidence for this interpretation. Honolulu maps to L = 1.17 and was located very near the dusk flank. The waveforms of the Pi2 observed by Honolulu correlate well with the V_x waveforms observed by P4 and P5 $\sim$ 80 seconds prior. This is consistent with the directly-driven scenario of Pi2 generation [*Kepko and Kivelson*, 1999] which postulates that the braking of periodic flows is responsible for Pi2 observed at low latitudes on the flank. The additional 20 second delay from the inferred time of braking to low latitude Pi2 suggests a fast mode speed of 2500 km/s in the inner magnetosphere.

[14] Magnetic field oscillations prior to the arrival of the flow can be seen in Figures 3e and 3g. These began around the time that the diffuse auroral form began to brighten. We suggest that these magnetic oscillations represent Alfvén waves propagating from further downtail, generated by an Earthward traveling flow burst. They represent the changed magnetospheric configuration that must be communicated to the ionosphere. The data do not support a local generation of these waves. If the waves were associated with a near-Earth process (e.g., current disruption), we would expect an ionospheric signature much closer to the onset arc, rather than one occurring at higher latitude propagating equatorward for 6 minutes.

[15] Using λ = 630.0 observations from the Gillam NORSTAR all-sky imager we have identified for the first time an equatorward moving auroral patch poleward of the onset arc location observed prior to auroral substorm onset. We have further connected the observed sequence of events into a model of substorm onset that is consistent with the recent results from *Angelopoulos et al.* [2008]. The sensitivity of the λ = 630.0 nm emissions to scattered plasmasheet

electrons makes these data a particularly sensitive indicator of plasmasheet dynamics. This relatively unexplored dataset has the potential to address gaps in our understanding of the coupling between plasmasheet dynamics and auroral activity. Left unresolved is the question of whether the increased λ = 630.0 emissions represent enhanced precipitating number flux or increased precipitation energy (or both). Future work to identify the process - or processes - responsible for the generation of the diffuse λ = 630.0 nm emissions is underway.

[16] **Acknowledgments.** We acknowledge NASA contract NAS5-02099 and V. Angelopoulos for use of data from the THEMIS Mission. Financial support of the FGM Lead Investigator Team at the Technical University of Braunschweig by the German Ministerium für Wirtschaft und Technologie and the Deutsches Zentrum für Luft- und Raumfahrt under grant 50QP0402 is acknowledged. Honolulu magnetometer data was provided by the USGS Geomagnetism Program. The authors thank I.R. Mann and the CARISMA team for the Fort Churchill data. CARISMA is operated by the University of Alberta and funded by the Canadian Space Agency. E. Spanswick thanks T. Trondsen for useful discussions.

References

Angelopoulos, V. (2008), The THEMIS Mission, *Space Sci. Rev.*, *141*, 453–476, doi:10.1007/s11214-008-9336-1.

Angelopoulos, V., et al. (2008), Tail reconnection triggering substorm onset, *Science*, *321*, 931–935, doi:10.1126/science.1160495.

Auster, H. U., et al. (2008), The THEMIS fluxgate magnetometer, *Space Sci. Rev.*, *141*, 235–264, doi:10.1007/s11214-008-9365-9.

Baker, D. N., T. I. Pulkkinen, V. Angelopoulos, W. Baumjohann, and R. L. McPherron (1996), Neutral line model of substorms: Past results and present view, *J. Geophys. Res.*, *101*, 12,975–13,010.

Birn, J., and M. Hesse (1996), Details of current disruption and diversion in simulations of magnetotail dynamics, *J. Geophys. Res.*, *101*, 15,345–15,358.

Donovan, E., et al. (2003), Auroral imaging in Canadian CANOPUS and NORSTAR programs, paper presented at the 30th Annual European Meeting on Atmospheric Studies by Optical Methods, Univ. Courses on Svalbard, Longyearbyen, Norway.

Eather, R. H., and S. B. Mende (1971), Airborne observations of auroral precipitation patterns, *J. Geophys. Res.*, *76*, 1746–1755.

Elphinstone, R. D., D. Hearn, J. S. Murphree, and L. L. Cogger (1991), Mapping using the Tsyganenko long magnetospheric model and its relationship to Viking auroral images, *J. Geophys. Res.*, *96*, 1467–1480.

Kepko, L., and M. Kivelson (1999), Generation of Pi2 pulsations by bursty bulk flows, *J. Geophys. Res.*, *104*, 25,021–25,034.

Kepko, L., M. G. Kivelson, R. L. McPherron, and H. E. Spence (2004), Relative timing of substorm onset phenomena, *J. Geophys. Res.*, *109*, A04203, doi:10.1029/2003JA010285.

McFadden, J. P., et al. (2008), The THEMIS ESA plasma instrument and in-flight calibration, *Space Sci. Rev.*, *141*, 277–302, doi:10.1107/s11214-008-9440-2.

Mende, S. B., C. W. Carlson, H. U. Frey, T. J. Immel, and J.-C. Gérard (2003), IMAGE FUV and in situ FAST particle observations of substorm aurorae, *J. Geophys. Res.*, *108*(A4), 8010, doi:10.1029/2002JA009413.

Mende, S. B., et al. (2008), The THEMIS array of ground based observatories for the study of substorms, *Space Sci. Rev.*, *141*, 357–387, doi:10.1007/s11214-008-9380-x.

Rees, M. H., and R. G. Roble (1986), Excitation of the O(^{1}D) atoms in aurorae and emission of the [OI] 6300-Å line, *Can. J. Phys.*, *64*, 1608–1613.

Samson, J. C., L. R. Lyons, P. T. Newell, F. Creutzberg, and B. Xu (1992), Proton aurora and substorm intensifications, *Geophys. Res. Lett.*, *19*, 2167–2170.

Sharp, W. E., M. H. Rees, and A. I. Stewart (1979), Coordinated rocket and satellite measurements of an auroral event: 2. Rocket observations and analysis, *J. Geophys. Res.*, *84*, 1977–1985.

Sharp, W. E., D. Ortland, and R. Cageao (1983), Concerning sources of 0(^{1}D) in aurora: Electron impact and dissociative recombination, *J. Geophys. Res.*, *88*, 3229–3232.

Shiokawa, K., et al. (1998), High-speed ion flow, substorm current wedge, and multiple Pi 2 pulsations, *J. Geophys. Res.*, *103*, 4491–4507.

Tsyganenko, N. A. (2002), A model of the near magnetosphere with a dawn-dusk asymmetry 2. Parameterization and fitting to observations, *J. Geophys. Res.*, *107*(A8), 1176, doi:10.1029/2001JA000220.

V. Angelopoulos, Institute of Geophysics and Planetary Physics, University of California, Los Angeles, CA 90095, USA.

E. Donovan and E. Spanswick, Department of Physics and Astronomy, University of Calgary, 2500 University Dr. NW, Calgary, AB T2N 1N4, Canada.

K.-H. Glassmeier, Institute of Geophysics and Extraterrestrial Physics, Technical University of Braunschweig, Mendelssohnstr. 3, D-38106 Braunschweig, Germany.

L. Kepko and J. Raeder, Space Science Center, University of New Hampshire, Morse Hall, 39 College Rd., Durham, NH 03842, USA. (larry.kepko@unh.edu)

J. McFadden, Space Sciences Laboratory, University of California, 7 Gauss Way, Berkeley, CA 94720, USA.

H. J. Singer, Space Weather Prediction Center, NOAA, 325 Broadway, Boulder, CO 80305, USA.